

Vibrational Features of Water at the Low-Density/High-Density Liquid Structural Transformations

Ramil M. Khusnutdinoff^a Anatolii V. Mokshin^a

^a*Department of Physics, Kazan (Volga region) Federal University,
Kremlevskaya Street 18, 420008 Kazan, Russia*

Abstract

A structural transformation in water upon compression was recently observed at the temperature $T = 277$ K in the vicinity of the pressure $p \approx 2\,000$ Atm [R.M. Khusnutdinoff, A.V. Mokshin, *J. Non-Cryst. Solids* **357**, 1677 (2011)]. It was found that the transformations are related with the principal structural changes within the first two coordination shells as well as the deformation of the hydrogen-bond network. In this work we study in details the influence of these structural transformations on the vibrational molecular dynamics of water by means of molecular dynamics simulations on the basis of the model Amoeba potential ($T = 290$ K, $p = 1.0 \div 10\,000$ Atm). The equation of state and the isothermal compressibility are found for the considered (p, T) -range. The vibrational density of states extracted for THz -frequency range manifests the two distinct modes, where the high-frequency mode is independent on pressure whereas the low-frequency one has the strong, non-monotonic pressure-dependence and exhibits a step-like behavior at the pressure $p \approx 2000$ Atm. The extended analysis of the local structural and vibrational properties discovers that there is a strong correlation between the primary structural and vibrational aspects of the liquid-liquid structural transformation related with the molecular rearrangement within the range of the second coordination shell.

Key words: Amoeba water model, molecular dynamics, equation of state, local isothermal compressibility, vibrational density of states

PACS: 61.20.Ja, 61.25.Em, 67.25.dt, 68.35.Rh

Email addresses: khrm@mail.ru (Ramil M. Khusnutdinoff),
anatolii.mokshin@mail.ru (Anatolii V. Mokshin).

1 Introduction

The physico-chemical features and soluble properties of water are of the central importance for life on our planet. However, despite of a knowledge of some properties at the ambient conditions that corresponds only to narrow part of water phase diagram, the inherent structural and dynamical properties are still far from to be completely understood, that motivates to perform a large number of experimental and theoretical investigations of water [1,2,3,4,5,6,7,8,9,10,11,12,13]. Water is known as a 'system' with a rich variety of anomalous behavior related with the different phase states. For example, in a solid state, water has at least fifteen crystalline forms, where four of these can coexist with the liquid phase, and a variety of the amorphous phases known as amorphous ices and polyamorphism [2,14,15].

One of the interesting features of water is related with the first-order like phase transition from low-density liquid (LDL) state to high-density liquid (HDL) state was reported in Ref. [16]. The hypothesis of a "liquid-liquid phase transition" in water was considered in a series of experimental, computational and theoretical studies (see, for example, Refs. [17,18,19] and references therein). As it was found, the difference between these liquid states is mainly provided by the structural properties. Namely, in the HDL, the local tetrahedrally coordinated hydrogen bond (HB) structure is not fully developed, whereas in the LDL, a more open, locally "ice-like" HB network is realized [1,3]. Both these liquid states are closely associated with the two amorphous phases observed experimentally in water: the low-density amorphous (LDA) and the high-density amorphous (HDA) ices, although locus of this "transition" is still debatable [15,18,19,20]. Remarkably, that a sharp jump in density (volume) is smoothed with the increase of temperature (or the decrease of pressure) and disappears completely, while LDL/HDL structural transformations still exists. It is interesting to note that the amorphous phase of water is also characterized by the "transition" from HDA ice to very high-density amorphous (VHDA) ice [21,22,23,24,25]. A schematic phase diagram of water, that treats qualitatively some empirical results, is given in Fig. 1. Above the critical temperature of the predicted LDL/HDL transition, the jump in volume (density) is absent, but the local structure changes completely with pressure. This is clear detected by the radial distribution function (for example, for oxygen atoms), $g_{OO}(r)$, where the first minimum disappears, while the second maximum and minimum changes by a minimum and maximum, respectively (see right panel in Fig. 1). It is significant to note that although a schematic phase diagram of water is known in general sense for an extensive (p,T) -range (see, for example, Fig. 1 in Ref. [25] and Fig. 4 in Ref. [26]), the exact boundary location between LDL and HDL is not well-defined as well as the smoothed LDL/HDL transformations range are still undetected. So, the problem associated with the structural transformation and its influence on microscopic dynamics of liquid

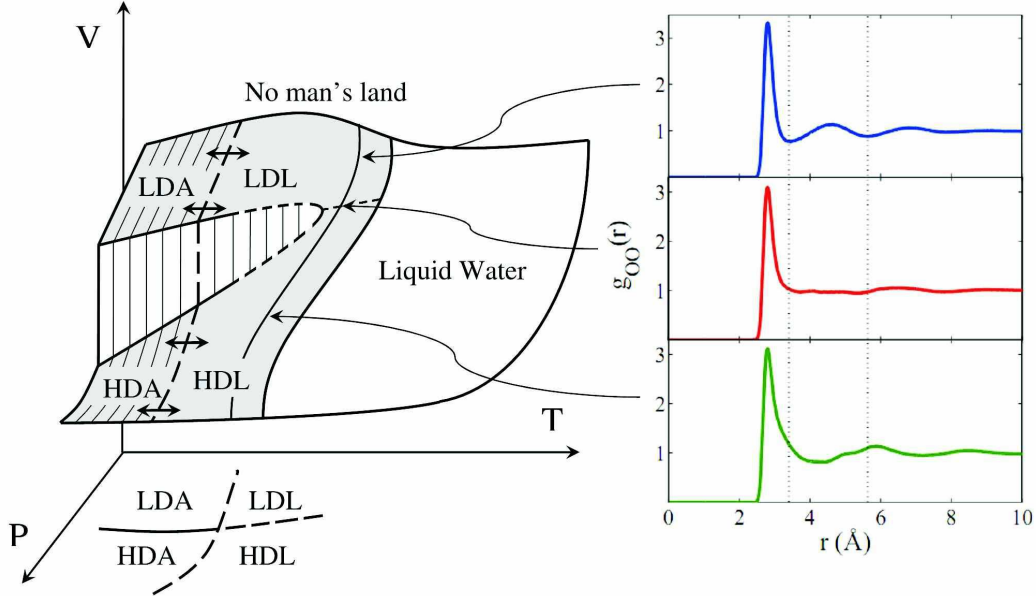


Figure 1. (Color online) Left panel: Schematic phase diagram of liquid-amorphous water (see also Ref. [27]). White range corresponds to a stable liquid water, gray region indicates the liquid-amorphous phase, which is characterized by the separated low-density and high-density states. Broken line is the conventional boundary between the liquid and the amorphous phases. Solid line is the 'isotherm' considered in the work, where a sharp jump in density is no observed. LDL/HDL-structural transformations arise at the temperature $T \in [260 \text{ K}; 400 \text{ K}]$ and the pressures $p \in [2000 \text{ Atm}; 4000 \text{ Atm}]$ (see Fig. 5 in Ref. [28] and Fig. 7 of Ref. [29]). Right panel: Radial distribution functions $g_{OO}(r)$ typical for three ranges of the phase diagram (LDL, LDL/HDL-boundary, HDL); the correspondence is indicated by arrows.

water (even at the room temperature) requires the additional studies [15]. The given work studies the structural features within first two coordination shells [30] as well as the vibrational properties of liquid water at the temperature $T = 290 \text{ K}$ and a wide range of pressure by means of molecular dynamics simulations on the basis of the Amoeba interaction potential. The correlation between structural features of the transformation and molecular vibrational dynamics of water is also considered.

This paper organized as follows. The details of molecular dynamics simulations of liquid water are presented in section 2. The structural transformations within the second coordination shell are explored by means of the local isothermal compressibility κ_T^0 in section 3. The manifestation of the effect of the structural transformations on the vibrational properties of water and the possible correlation between these both are also discussed here. Finally, we conclude with a short summary.

2 Simulation Details

Equilibrium classical molecular dynamics (MD) simulations of water at the constant temperature $T = 290$ K and the different pressures were performed on the basis of the Amoeba¹ (Atomic Multipole Optimized Energetics for Biomolecular Applications) water model suggested recently by Ren and Ponder [32,33]. The model uses a polarizable atomic multipole description of electrostatic interactions, where the polarization is treated due to the self-consistent induced atomic dipoles [32], and a modified version of the Thole's interaction model is used to damp the induction at a short range [34,35]. Our computations were performed for 4000 water molecules interacted within a cubic box with the periodic boundary conditions in all directions. The Ewald summation was used to handle the electrostatic interactions. Moreover, an atom-based switching window of the size 12 Å was applied to cut off the van der Waals interactions. The equations of motion were integrated via a modified Beeman algorithm [36],

$$\begin{aligned}\vec{r}(t + \Delta\tau) &= \vec{r}(t) + \vec{v}\Delta\tau + \frac{1}{6}\left(4\vec{a}(t) - \vec{a}(t - \Delta\tau)\right)\Delta\tau^2 + \mathcal{O}(\Delta\tau^4), \\ \vec{v}(t + \Delta\tau) &= \vec{v}(t) + \frac{1}{12}\left(5\vec{a}(t + \Delta\tau) + 8\vec{a}(t) - \vec{a}(t - \Delta\tau)\right)\Delta\tau + \mathcal{O}(\Delta\tau^3),\end{aligned}$$

with the time step $\Delta\tau = 1.0$ fs. The isothermal-isobaric ensemble at the temperature $T = 290$ K and the pressure $p = 1.0, 1000, 2000, 2500, 3000, 3750, 5000, 7797$ and $10\ 000$ Atm was applied by means of the Berendsen thermostat and barostat [37]. According to this scheme, to enforce the constant temperature the system was weakly coupled to a heat bath with some temperature. The velocities were scaled at an each step by such a way, that the rate of the temperature change is

$$\frac{dT}{dt} = \frac{T_0 - T}{\tau}. \quad (1)$$

¹ Recently, it was shown in Ref. [1], that the results of molecular dynamics simulations on the basis of Amoeba interaction potential for structural and dynamical properties of water are in a good agreement with the results on ab-initio molecular dynamics simulations as well as the experimental data on neutron diffraction [31] and inelastic X-ray scattering [6]. Note that the Amoeba model reveals for the isobar $P = 1.0$ Atm the maximum in density at the temperature $T = 290$ K instead of the well-known value 277 K [32]. Actually, one notices that the Amoeba potential does not reproduce the experimental equation of state correctly: for instance, the density 1.21 g/cm^3 at 290 K is reached at 5000 Atm in the present simulation, instead of 8000 Atm in the experiment.

where τ is the coupling parameter, which determines how tightly the bath and the system are coupled together, T_0 is the temperature of the external heat bath. This method provides an exponential decay of the system temperature towards the desired value. The change in temperature between the successive time steps is

$$\Delta T = \frac{\Delta\tau}{\tau} \left(T_0 - T(t) \right), \quad (2)$$

here

$$T(t) = \frac{1}{(3N - N_c)k_B} \sum_{i=1}^N \frac{\vec{p}_i^2}{m_i} \quad (3)$$

the instantaneous value of the temperature; N_c is the number of constraints and $(3N - N_c)$ is the total number of degrees of freedom. Thus, the scaling factor for the velocities is

$$\lambda = \sqrt{1 + \frac{\Delta\tau}{\tau} \left(\frac{T_0}{T(t) - 1} \right)}. \quad (4)$$

Within the Berendsen barostat the system is made to obey the equation of motion

$$\frac{dp}{dt} = \frac{p_0 - p}{\tau}, \quad (5)$$

where p_0 is the value of the applied pressure, p is the instantaneous system pressure. In the isotropic case, the box volume is scaled by a factor η , whereas the coordinates are scaled by $\eta^{1/3}$, where

$$\eta = 1 - \frac{\beta\Delta\tau}{\tau}(p_0 - p) \quad (6)$$

and β is the isothermal compressibility of the system. The value of the coupling parameter τ in our simulations was equal to 0.1 ps.

3 Results

3.1 Equation of State and Local Structural Properties

A central place at the study of any phase transition or structural transformations takes the consideration of the equation of states. Here, the equation of state was defined for the considered water model at the fixed temperature $T = 290$ K and different pressures. Results are shown in Fig. 2. As can be seen from the figure, the presented isotherm $\rho(p)$ is well fitted by the cubic polynomial

$$\rho(p) = c_0 + c_1p + c_2p^2 + c_3p^3, \quad (7)$$

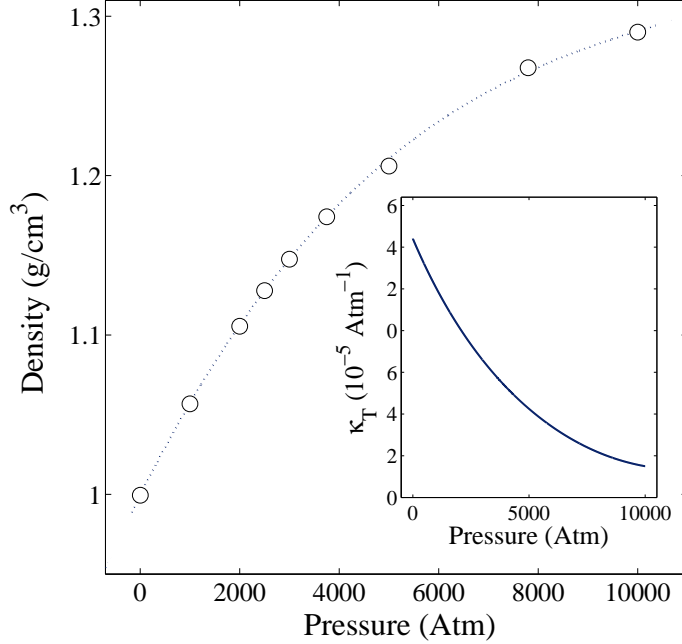


Figure 2. (Color online) Main: Equation of state for liquid water at the temperature $T = 290$ K. Inset: Pressure dependence of the isothermal compressibility κ_T .

Table 1

Parameters of equation (7) of liquid water at the temperature $T=290$ K.

Coefficients	290 K
c_0 (g/cm ³)	0.9996
c_1 (g/cm ³ · Atm ⁻¹)	$6.204 \cdot 10^{-5}$
c_2 (g/cm ³ · Atm ⁻²)	$-4.642 \cdot 10^{-9}$
c_3 (g/cm ³ · Atm ⁻³)	$1.349 \cdot 10^{-13}$

the values of the parameters c_0 , c_1 , c_2 , c_3 are given in Table 1. The obtained equation allows one to find directly the isothermal compressibility κ_T as

$$\kappa_T = \frac{1}{\rho} \left(\frac{\partial \rho}{\partial p} \right)_T. \quad (8)$$

There is no any visible singularity in the density $\rho(p)$ as well as in the isothermal compressibility $\kappa_T(p)$ (see inset of Fig. 2) in the vicinity of the pressure $p_c \simeq 2000$ Atm, where LDL/HDL-structural transformations were observed [1]. This is direct evidence of the absence of the first-order-like transition at LDL/HDL structural transformations, while in amorphous ices this transition exists [27].

To perform a detailed study at microscopic level, we suggest to consider the

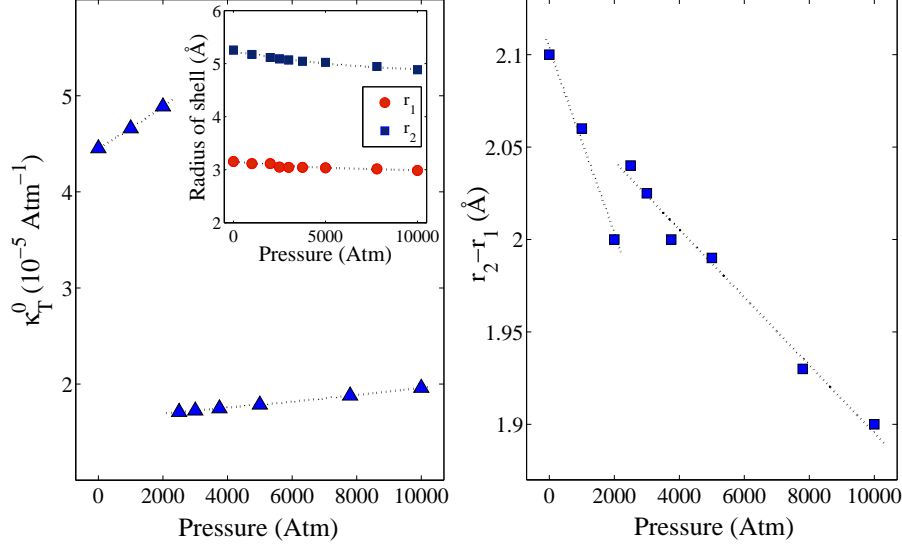


Figure 3. (Color online) Main: Pressure dependence of the local isothermal compressibility κ_T^0 (left panel) and the difference $(r_2 - r_1)$ (right panel). Inset: Radius of the first two coordination shells vs. pressure.

features upon the local spatial ranges around a water molecule within the boundaries of the closest coordination shells. For water the first two coordination numbers defined as [38]

$$N(r_c) = 4\pi n \int_0^{r_c} r^2 g(r) dr, \quad (9)$$

take the values $N(r_1) = 4$ and $N(r_2) = 16$, where r_1 and r_2 is the radius of the first and the second coordination shell, respectively; n is the oxygen-number density. Therefore, on the basis of Eq. (9) the sizes of the first two coordination shells r_1 and r_2 can be found for an arbitrary condensed phase as the distances, where $N(r_1) = 4$ and $N(r_2) = 16$. Then, the local, short-ranged properties can be extended to these of the spherical layer enclosed between r_1 and r_2 of the volume $V_0 = (4\pi/3)(r_2^3 - r_1^3)$. The isothermal compressibility extended to the *local* volume will be defined as

$$\kappa_T^0 = -\frac{1}{V_0} \left(\frac{\partial V_0}{\partial p} \right)_T. \quad (10)$$

Fig. 3 presents the pressure dependence of these characteristics: the local isothermal compressibility κ_T^0 ; the radius of the first two coordination shells r_1 and r_2 , and the difference $(r_2 - r_1)$ associated with the linear size of the considered local range. Contrary to the isothermal compressibility κ_T (inset of Fig. 2), which has a nonlinear monotonic decrease with pressure, the local isothermal compressibility κ_T^0 demonstrates a significant jump at the pressure $p_c \approx 2000$ Atm. A peculiarity in the vicinity of this value of pressure is also clear observed for the difference $r_2 - r_1$ presented in Fig. 3, although it is not

so obvious in the dependencies $r_1(p)$ and $r_2(p)$. Such result is a direct evidence that the structural transformations from LDL to HDL in water at the pressure $p_c \approx 2000$ Atm are related with the structural rearrangement within the second coordination shell. Then, the next question arises naturally: Have these structural transformations an influence on the inherent microscopic dynamics? One of the simplest way to answer on the question is to consider the vibrational density of states of the system.

3.2 Vibrational Density of States

The vibrational density of states (VDOS) characterizes the distribution over frequencies related with the molecular vibrational degree of freedom [39]:

$$\tilde{\Phi}(\omega) = \frac{1}{2\pi} \left[\int_{-\infty}^{\infty} \frac{\langle \vec{v}(0) \cdot \vec{v}(t) \rangle}{\langle \vec{v}(0) \cdot \vec{v}(0) \rangle} e^{i\omega t} dt \right]^2, \quad (11)$$

where $\vec{v}(t)$ is the velocity of the mass center of a molecule at the time t . Fig. 4 presents the defined VDOS of liquid water at the different pressures and the fixed temperature $T = 290$ K. As can be seen, VDOS has a bimodal form for all the cases. It is remarkable that the high-frequency peak position in VDOS is independent on pressure whereas the low-frequency peak changes both the intensity and the position ω_s . As can be see from the pressure dependence of ω_s given in inset (a) of Fig. 4, the quantity ω_s has a non-monotonic step-like behavior in vicinity of the characteristic value of pressure $p_c \approx 2000$ Atm. This indicates on the correlation of the low-frequency molecular vibrational properties with the structural transformations at the pressure. While high-frequency mode corresponds to the inherent vibrational processes of the molecules, the time scale $\tau_s \sim 1/\omega_s$ is related with the vibrational dynamics of the molecular conglomerates [40,41]. The immediate correlation of the low-frequency vibrations with the structural transformations at the local spatial scales in the range of the second coordination shell can be directly seen from inset (b) of Fig. 4. Recently, we have shown [1] that the increase of pressure gives rise the monotonic decrease of the tetrahedral order parameter, since the spatial structures of the five bonded water molecules changes. The low-frequency mode can be attributed to the vibrational motions of the separate molecular tetrahedral complexes. So, one can concluded that the pressure-induced changes in the low-frequency mode is governed by the change of geometry of the local molecular conglomerates formed by five bonded molecules.

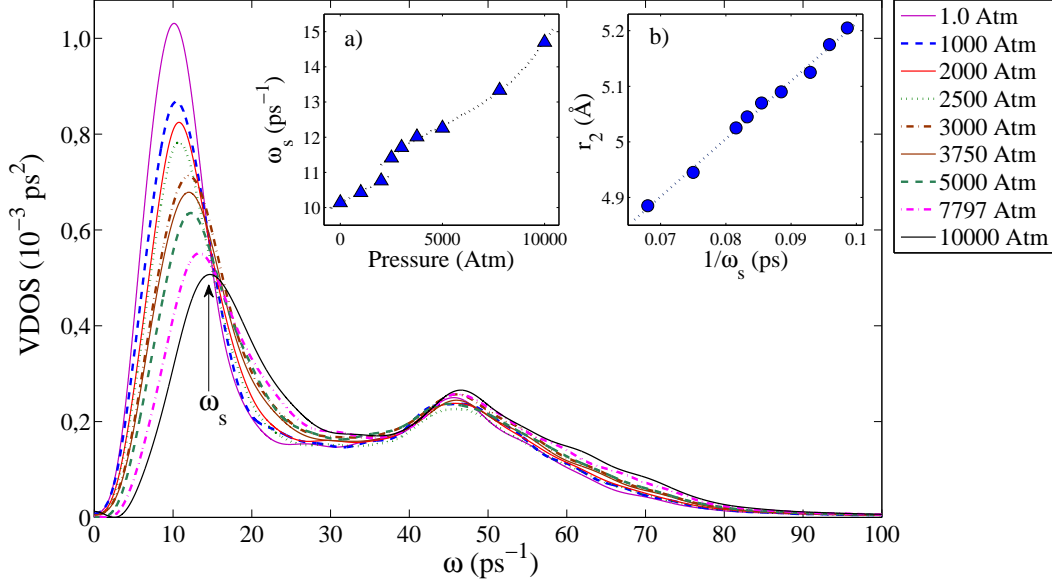


Figure 4. (Color online) Main: Vibrational density of states of liquid water at the temperature $T = 290$ K. Inset: (a) Pressure dependence of the low-frequency peak in VDOS indicated by arrow on main panel; (b) Radius of the second coordination shell r_2 vs. characteristic time scale associated with the low-frequency vibrational dynamics, $1/\omega_s$, for liquid water at the temperature $T = 290$ K.

4 Summary

Results of this study suggest explicitly the existence of the structural transformations from low-density state to high density one at a “stable liquid region” of the water phase diagram. Namely, we found for water system at the temperature 290 K that the Amoeba model reveals the transformation in the vicinity of the characteristic value of pressure $p_c \approx 2000$ Atm. It is necessary to note the corresponding structural transformation from LDL to HDL water is not marked in the temperature-pressure phase diagrams of water given recently, for example, in Ref. [2] (see Fig. 1) and Ref. [26] (Fig. 4).

Strikingly, the transformation considered in this work has a lot of similar features with the *polyamorphic* phase transition from the low- to high-density amorphous forms of ice, which has been experimentally observed near 2000 Atm and recognized as a first-order like transition (see work of O. Mishima et al. [27]). Furthermore, the transition in amorphous phase has a peculiarity to involve the movement of one water molecule from the second coordination shell to an interstitial site in the first coordination shell [22,42], that is very similar to LDL/HDL structural transformation considered here. Nevertheless, in the studied temperature-pressure range of stable liquid phase, there is no signatures of a phase transition in the thermodynamic sense between these two forms of water.

The isothermal compressibility κ_T of the system decreases steadily with pressure, while the local extension of the isothermal compressibility κ_T^0 as well as other local structural and vibrational characteristics manifests a step-like behavior at the characteristic value of pressure $p_c \approx 2000$ Atm. It is found that the LDL/HDL structural transformation in the vicinity of the pressure $p_c \approx 2000$ Atm has an influence on the low-frequency vibrational dynamics whereas the high-frequency molecular dynamics is independent on the pressure. Moreover, there is a strong correlation between low-frequency vibrational dynamics and the spatial scale of the second coordination shell.

5 Acknowledgments

This work was supported by grant of the Russian Foundation for Basic Research and the Centre National de la Recherche Scientifique (No. 09-02-91053-CNRS-a).

References

- [1] R.M. Khusnutdinoff, A.V. Mokshin, *J. Non-Cryst. Solids* **357**, 1677 (2011).
- [2] A.K. Soper, *Mol. Phys.* **106**, 2053 (2008).
- [3] A.K. Soper and M.A. Ricci, *Phys. Rev. Lett.* **84**, 2881 (2000).
- [4] Y. Katayama, T. Hattori, H. Saitoh et al, *Phys. Rev. B* **81**, 014109 (2010).
- [5] K. Davitt, E. Rolley, F. Caupin, A. Arvengas, and S. Balibar, *J. Chem. Phys.* **133**, 174507 (2010).
- [6] M. Krisch, P. Loubeyre, G. Ruocco et al, *Phys. Rev. Lett.* **89** 125502 (2002).
- [7] H. Jansson, R. Bergman, and J. Swenson, *Phys. Rev. Lett.* **104**, 017802 (2010).
- [8] L. Liu, A. Faraone, S.-H. Chen, *Phys. Rev. E* **65**, 041506 (2002).
- [9] F. Li and J.L. Skinner, *J. Chem. Phys.* **133**, 244504 (2010).
- [10] E.B. Moore and V. Molinero, *J. Chem. Phys.* **132**, 244504 (2010).
- [11] A.K. Soper and C.J. Benmore, *Phys. Rev. Lett.* **101**, 065502 (2008).
- [12] C. Vega, J.L.F. Abascal, M.M. Conde and J.L. Aragonés, *Faraday Discuss.* **141**, 251 (2009).
- [13] D. Paschek, *Phys. Rev. Lett.* **94**, 217802 (2005).

- [14] C.G. Salzmann, P.G. Radaelli, E. Mayer, and J.L. Finney, *Phys. Rev. Lett.* **103**, 105701 (2009).
- [15] I. Brovchenko, A. Oleinikova, *Chem. Phys. Chem.* **9**, 2660 (2008).
- [16] P.H. Poole, F. Sciortino, U. Essmann and H.E. Stanley, *Nature (London)* **360**, 324 (1992).
- [17] O. Mishima and H.E. Stanley, *Nature* **396**, 329 (1998).
- [18] P.G. Debenedetti, *J. Phys.: Condens. Matter* **15**, R1669 (2003).
- [19] P.G. Debenedetti and H.E. Stanley, *Phys. Today* **56**, 40 (2003).
- [20] T. Loerting, C.G. Salzmann, K. Winkel, E. Mayer, *Phys. Chem. Chem. Phys.* **8**, 2810 (2006).
- [21] T. Loerting, C. Salzmann, I. Kohl, E. Mayer, and A. Hallbrucker, *Phys. Chem. Chem. Phys.* **3**, 5355 (2001).
- [22] J.L. Finney, A. Hallbrucker, I. Kohl, A.K. Soper, D.T. Bowron, *Phys. Rev. Lett.* **88**, 225503 (2002).
- [23] J.L. Finney, D.T. Bowron, A.K. Soper, T. Loerting, E. Mayer, and A. Hallbrucker, *Phys. Rev. Lett.* **89**, 205503 (2002).
- [24] T. Loerting, W. Schustereder, K. Winkel, C. Salzmann, I. Kohl, E. Mayer, *Phys. Rev. Lett.* **96**, 025701 (2006).
- [25] K. Winkel, M.S. Elsaesser, E. Mayer, T. Loerting, *J. Chem. Phys.* **128**, 044510 (2008).
- [26] H.E. Stanley, P. Kumar, L. Xu et al, *Physica A* **386**, 729 (2007).
- [27] O. Mishima, *J. Chem. Phys.* **133**, 144503 (2010).
- [28] A.M. Saitta and F. Datchi, *Phys. Rev. E* **67**, 020201(R) (2003).
- [29] F.Li, Q. Cui, Z. He, T. Cui et al, *J. Chem. Phys.* **123**, 174511 (2005).
- [30] A.V. Mokshin, R.M. Yulmetyev, and P. Hänggi, *Phys. Rev. Lett.* **95**, 200601 (2005).
- [31] A.K. Soper, *Chem. Phys.* **258**, 121 (2000).
- [32] P. Ren and J.W. Ponder, *J. Phys. Chem. B* **107**, 5933 (2003).
- [33] P. Ren and J.W. Ponder, *J. Phys. Chem. B* **108**, 13427 (2004).
- [34] B.T. Thole, *Chem. Phys.* **59**, 341 (1981).
- [35] J.W. Ponder, *TINKER: Software Tools for Molecular Design*; 4.1 ed.: Washington University School of Medicine: Saint Louis, (2003).
- [36] M.P. Allen and D.J. Tildesley, *Computer Simulation of Liquids*, Clarendon Press, Oxford (1987).

- [37] H.J.C. Berendsen, J.P.M. Postma, W.F. van Gunsteren, A. DiNola, J.R. Haak, *J. Chem. Phys.* **81**, 3684 (1984).
- [38] Zh. Yan, S.V. Buldyrev, P. Kumar, N. Giovambattista, P.G. Debenedetti, H.E. Stanley, *Phys. Rev. E* **76**, 051201 (2007).
- [39] J. Kohanoff, *Comp. Mat. Sci.* **2**, 221 (1994).
- [40] M. Heyden, J. Sun, S. Funkner, G. Mathias, H. Forbert, M. Havenith, D. Marx, *Proc. Natl. Acad. Sci.* **107**, 12068 (2010).
- [41] A.V. Mokshin and J.-L. Barrat, *Phys. Rev. E* **82**, 021505 (2010).
- [42] D.T. Bowron, J.L. Finney, A. Hallbrucker, I. Kohl, T. Loerting, E. Mayer, A.K. Soper, *J. Chem. Phys.* **125**, 194502 (2006).